African Journal of Advanced Pure and Applied Sciences (AJAPAS)
Online ISSN: 2957-644X
Volume 3, Issue 3, 2024, Page No: 183-196
Website: *https://aaasjournals.com/index.php/ajapas/index*
معامل التأثير العربي 2023: (1.55) **SJIFactor 2023: 5.689** **ISI 2022-2023: 0.557**
Special issue: First Libyan Conference on Technology and Innovation (LCTI-2024), Benghazi, Libya

Thermodynamics, Isotherms, and Kinetics Evaluation of the (Nickel Oxide/Cerium Dioxide/Graphene Oxide Nanocomposite) for Methylene Blue (MB) Dye Removal

Mohammed A. Al-Madani [1 *], Salah A. Gnefid [2], Faraj M. Al-Lafi [3]
[1] Materials and Corrosion Eng. Dep., Eng. Faculty, Sebha University, Sebha, Fazzan, Libya
[2] Mining Eng. Dep., Natural Resources Faculty, Sawknah, Al-Joufra, Libya
[3] Materials Dep., Eng. Faculty, Missouri University, Kanas, Missouri, India

تقييم الديناميكا الحرارية والأيسوثرم والحركية (لأكسيد النيكل/ثاني أكسيد السيريوم/المركب النانوي لأكسيد الجرافين) لإزالة صبغة الميثيلين الزرقاء

محمد الكيلاني المدني[1*]، صالح عبدالله قنيفيد[2]، فرج محمد اللافي[3]
[1] قسم هندسة المواد والتآكل، كلية الهندسة، جامعة سبها، سبها، ليبيا
[2] قسم هندسة التعدين، كلية الموارد الطبيعية، جامعة الجفرة، سوكنة، ليبيا
[3] قسم المواد، كلية الهندسة، جامعة ميسوري، كاناس، الهند

[*]Corresponding author: moh.ibrahim@sebhau.edu.ly

Received: March 10, 2024	Accepted: May 05, 2024	Published: May 10, 2024

Abstract

Serious environmental issues are brought on by the textile industry's excessive growth, consumption of water and dyes, particularly when it comes to excessive water body pollution. When it comes to green chemistry, adsorption is an appealing, workable, affordable, highly effective, and sustainable method for removing contaminants from water. In this research paper, Graphene oxide/nickel oxide/cerium dioxide nanocomposite ($NiO/CeO_2/GO$): kinetics, isotherms, and thermodynamics of adsorption behaviour method for Methylene Blue (MB) elimination from water-based solutions was examined. Langmuir, Freundlich, and Dubinin-Radushkevich isotherms were used to assess the equilibrium data. The Langmuir model provides the best explanation for the uptake of (MB) dye, suggesting that the adsorption of (MB) dyes onto ($NiO/CeO_2/GO$) nano-composites is monolayer and uniform. Direct dye adsorption is found to follow pseudo-first-order and pseudo-second-order models, respectively, based on an analysis of the adsorption kinetics. In the response surface methodology-determined optimal removal setting (pH 7, contact time 40 min), the maximum adsorption capacity was (105.26 mg/g). Adsorption uptake was shown to increase with increases of initial dye concentration and contact time. Furthermore, the process demonstrated endothermic nature. Changes in entropy, enthalpy, and Gibb's free energy were (0.031, 0.073) kJ/mol.K, and -21.66 kJ/mol, respectively. The (MB) dye removal from aqueous solutions was quickly and effectively by comparing the results with those that have been published.

Keywords: (MB) Dye, ($NiO/CeO_2/GO$) Nano-Composites, Isotherms, Asorption Kinetics, Thermodynamics.

الملخص

نتيجة للتزايد المفرط في صناعات النسيج والأستهلاك المتزايد للمياه والأصباغ حالياً, نجم عن ذلك الكثيرمن المشاكل البيئية الخطيرة، ومنها على سبيل المثال تلوث المسطحات المائية. عندما يتعلق الأمر بالعمليات الكيميائية التي تقلل من أو تلغي إنتاج أو توليد المواد الخطرة (ما يسمى بالكيمياء الخضراء)، فإن طريقة الامتزاز تعتبر طريقة عملية وفعالة وبتكاليف معقولة

لإزالة الملوثات من المحاليل المائية. في هذا البحث، تم أختبار عملية إمتزاز صبغة الميثيلين الزرقاء بواسطة المركب النانوي (أكسيد الجرافين / أكسيد النيكل / المركب النانوي ثاني أكسيد السيريوم) وذلك بأستخدام آلية الإمتزاز والنماذج الإيزوثيرمية ومعاملات الديناميكا الحرارية. تم استخدام ثلاث نماذج أيزوثيرمية: لانجمير وفروندليتش ودوبينين-رادوشكيفيتش. وكان نموذج لانجمير هو أفضل النماذج التي تم أستخدامها لتفسير سلوك عملية الإمتزاز، وهذا يدل أن عملية الإمتزاز على سطح المركب النانوي أحادية الطبقة ومتجانسة على السطح. بناءً على نتائج آلية الإمتزاز, وجد أن عملية الإمتزاز المباشرة لصبغة الميثلين الزرقاء تتبع نماذج الدرجة الأولى الغير حقيقية وكذلك الدرجة الثانية الغير حقيقية على التوالي, وكانت أقصى سعة أمتزاز لصبغة الميثيلين الزرقاء تم الحصول عليه من النتائج هو (105.26 ملجم\جم) عند رقم هيدروجيني (7) وخلال زمن تلامس (40 دقيقة). وتبين أن عملية أمتزاز صبغة الميثيلين الزرقاء تزداد طردياً مع زيادة التركيز الأولي للصبغة وكذلك مع زيادة زمن التلامس مع السطح. أظهرت نتائج معاملات الديناميكا الحرارية أن عملية الإمتزاز كانت ماصة للحرارة وليست طاردة لها, حيث تراوحت قيم التغيرفي الطاقة الحرة والطاقة الداخلية الكامنة والأنتروبيا: (-21.66 و0.031 كيلوجول\مول و0.073 كيلوجول\مول.كيلفن) على التوالي. من خلال مقارنة النتائج المتحصل عليها في هذا البحث مع بعض نتائج بعض البحوث التي تم نشرها مسبقاً تبين أن عملية إمتزاز صبغة الميثيلين الزرقاء في هذا البحث بواسطة المركب النانوي المستخدم كان سريعة وفعالة نسبياً.

الكلمات المفتاحية: صبغة الميثيلين الزرقاء، أكسيد الجرافين/أكسيد النيكل/ثاني أكسيد السيريوم، الأيزوثيرمات، آلية الإمتزاز، الديناميكا الحرارية.

Introduction

Because dye contaminants have complicated molecular structures and are not biodegradable, their presence in textile wastewaters is a major cause for concern [1]. The presence of metals, aromatics, and other substances in dye pollutants' structures can make them hazardous and detrimental to the environment, as well as negatively impact aquatic photosynthetic processes. Furthermore, dyes can lead to major health problems in people, including problems with the kidneys, liver, and central nervous system. Chromosome breakage, respiratory issues, carcinogenesis, and mutagenicity are a few effects of excessive dye concentration in the environment [2].

Methylene blue (MB) is one of the most widely used chemicals in industry; it can induce bluish skin pigmentation, cyanosis, and irritation of the skin, eyes, and respiratory tract. Nonetheless, a variety of industrial processes, like textile production, release tones of wastewater into the environment each year [3]. Eliminating colours from industrial effluents is a crucial step in pollution prevention, particularly for textile companies [4].

Due to their resistance to photodegradation and biodegradation, (MB) dye molecules and present difficulties for the treatment procedures when present in textile effluent [5]. Nevertheless, the adsorption approach has demonstrated a great deal of promise as the preferred technique for the removal of (MB), particularly because of its quick adsorption kinetics, ease of design and use, and inexpensive cost [6].

Single-phase, two-phase, or three-phase materials with a size less than 100 nm are called nano-composites [7]. Researchers can use nanoparticles in a wide range of sectors, including the textile industries, due to their known various physical and chemical characteristics [8].

Cerium oxide (CeO_2) has many unique qualities that make it a common ingredient in many different applications. These properties include a high capacity for storing oxygen, the ability to exist in two states of oxidation (Ce^{4+} and Ce^{3+}), an abundance of oxygen vacant positions, and redox reactions between (Ce^{4+} and Ce^{3+}) [9].

Graphene, a carbon-based nanostructured material, has special qualities of its own. For example, it can act as a co-catalyst in nanocomposites as well as a conducting carrier, adsorbent, photosensitizer, and photo stabilizer [10]. Graphene serves as the fundamental building block for all other dimensional graphitic compounds and is regarded as the founding element of certain carbon allotropes [11]. Similar to graphene, graphene oxide (GO) has functional groups that incorporate oxygen [12]. GO structures include oxygen-based functional groups that allow the material to dissolve in water, such as carbonyl (C=O), hydroxide (–OH), carboxyl (–COOH), and epoxide (C–O–C) [13]. Dye removal is one of the many possible uses for GO-based composites in the energy and environmental domains [14].

The most important type of data required to comprehend an adsorption process is, notably, adsorption equilibrium data [15]. The adsorption process is therefore dependent on the chemical reaction between the adsorbent and the adsorbate dye solutions at equilibrium. Based on potential surface chemistry that may exist

between the adsorbent and MB dye molecule, a variety of adsorbents have been developed with the primary objective of selectively interacting with the target MB dye molecules [16].

The primary goals of this work are to use thermodynamic parameters, isotherm models, and kinetics to study the adsorption of NiO/CeO_2-GO nanocomposites as an adsorbent for the removal of (MB) dye from aqueous solutions. Furthermore, the synthesized nanomaterial was taken into consideration in an earlier study [17], which employed a range of spectroscopic techniques to analysis the NiO/CeO_2-GO nanocomposite adsorbent, including SEM, FTIR, Romans Spectroscopy, Photo Luminescence (PL), and Dynamic Light Scattering (DLS).

(MB) from wastewater has been adsorbed using a variety of materials in recent years. In 2024, Atef El Jery, et al. [18], set out to optimize the methylene blue dye wastewater treatment process by developing a cost-effective and environmentally friendly technique and by learning more about the kinetics and thermodynamics of the adsorption process. Using rice straw as the precursor, an adsorbent with selective methylene blue dye adsorption properties was created. In order to fill in knowledge gaps and improve comprehension of adsorption mechanisms, experimental investigations were carried out to explore the adsorption isotherms and models under diverse process conditions. A number of adsorption isotherm models were used to conceptually explain the adsorption mechanism, including Temkin, Freundlich, Langmuir, and Langmuir–Freundlich. The computed equilibrium adsorption capacity (qe) showed good agreement with the experimentally obtained data, according to equilibrium thermodynamic results. With potential uses beyond this particular dye type, the study's findings offer insightful information about the thermodynamics and kinetics of methylene blue dye adsorption. A unique and affordable method for removing (MB) dye from wastewater is to use rice straw as an adsorbent material.

In 2023, Al-Madani and Al-Lafi [17], developed a NiO/CeO_2-GO nanocomposite by a hydrothermal method; it was examined by means of XRD, FTIR, SEM, Roman Spectroscopy (RS), Photo Luminescence Spectra (PL), and Dynamic Light Scattering (DLS) methods. It was shown that the adsorption of Methylene Blue (MB) is increased upon the addition of GO. The greatest removal of (MB) from an aqueous solution was determined to be 93.22% under the optimal conditions of pH (5), contact duration of (40 minutes), and NiO/CeO_2-GO (1.00 mg/L).

In 2023, Tshimangadzo S. Munonde, et. al. [19], examined using the MnO_2@reduced graphene oxide (rGO) adsorbent the adsorptive removal of methylene blue dye, which is frequently used in the textile industry. With a maximal adsorption capacity of 156 mg/g, the Langmuir isotherm model best explained the equilibrium experimental results, indicating a monolayer adsorption. The pseudo-second order kinetic model was best matched by the kinetic data, indicating a chemisorption adsorption mechanism. The adsorption process's practicality, unpredictability, and spontaneous nature were validated by the thermodynamic data ΔG^o, ΔH^o, and ΔS^o. MnO_2@rGO nanocomposite was used to remove methylene blue from spiking textile wastewater, and the removal rate was 98–99%.

In 2022, Abbas M. Abbas, et. al. [20], prepared a new nanocomposite (HBS) prepared based on humic acid, biochar, and silica using the co-precipitation method for methylene blue dye removal from industrial wastewater. The humic acid, biochar, and silica are produced from compost, tomato residual, and Rice husk feedstocks. The optimum conditions for removing methylene blue from wastewater are 50 mg of (HBS), 100 mg/L (initial concentration), pH 9, and contact time of 60 min at room temperature. The adsorption process was endothermic and fitted with the Langmuir model. The maximum adsorption capacity was 16.23 mg/g. The created a new nanocomposite (HBS) for the removal of methylene blue dye from industrial wastewater. It was based on humic acid, biochar, and silica and was made utilizing the co-precipitation process. Rice husk feedstocks, compost, and tomato leftovers are used to make silica, charcoal, and humic acid. The ideal parameters for eliminating methylene blue from wastewater are 50 mg of (HBS), 100 mg/L (starting concentration), pH 9, and 60 minutes of room temperature contact time. The Langmuir model was able to suit the endothermic adsorption process. 16.23 mg/g was the greatest adsorption capacity. The spontaneous process of adsorption is indicated by a negative value of ΔG^o. Three cycles of effective regeneration of the (HBS) nanocomposite were achieved for the elimination of (MB).

In 2022, Davoudi and Shahnaz [21], examined if the produced NiO-SiO_2NPs might be used as a new adsorbent to remove the colour Methylene Blue (MB) from aqueous solutions. The analysis demonstrated the suitability of NiO-SiO_2NPs as an affordable, readily available adsorbent for the effective extraction of (MB) dye from aqueous solutions. The Langmuir isotherm has good applicability for explaining experimental data, with maximum adsorption capacity of the (MB) dye for SiO_2 and NiO-SiO_2NPs being approximately 117.0 and 140.0 mg/g, respectively. The experimental equilibrium data were fitted to the conventional isotherm models. Adsorption kinetics were studied using kinetics experiments, and the pseudo-second-order kinetics and the kinetic outcomes agreed pretty well. When the temperature of the adsorption process was taken into consideration, the thermodynamic behavior of the process was examined. The findings indicated that the process is exothermic (ΔH^o

< 0) and spontaneous ($\Delta G^o < 0$) at the employed temperature range ($\Delta S^o < 0$). Conclusion: The investigated adsorption process is physisorption based on the magnitude of ($\Delta H^o < 0$).

In 2021, Kashma Sharma, et. al. [22], shown the creation of gold (Au)/hydroxyapatite (HA) nanocomposites to boost the wastewater's ability to adsorb methylene blue (MB) dye. via H_3PO_4 and $Ca(OH)_2$ as starting ingredients, HA nano-powder was created via a wet chemical precipitation process. Batch tests were performed on the synthesized composite to conduct adsorption studies. The kinetic modelling results showed that the pseudo-first-order kinetic model precisely matches the experimental data. Pseudo-first-order and pseudo-second-order models were employed to suit the kinetic data. The obtained results suggest that the synthesized sample is suitable to be used as an adsorbent for the efficient removal of (MB) dye from wastewater.

In 2021, W. A. Albokheet, et. al. [23], produced the nickel oxide-carboxymethyl cellulose (NiO/CMC) nanocomposite using the co-precipitation technique in order to extract the colour methylene blue (MB) from drains. Data were compared using the pseudo-second-order equation and the Langmuir model, respectively, and the adsorption kinetics, equilibrium isotherms, and thermodynamics were examined. In addition, ΔG^o, ΔH^o, and ΔS^o were computed; the resulting graphical abstract (NiO/CMC) suggested that the adsorption of (MB) via the produced (Ni/CMC) nanocomposite was an endothermic and spontaneous process.

In 2020, Thaisa Caroline Andrade Siqueira [24], was to investigate how sugarcane bagasse (SCB) would adsorb the colorant methylene blue (MB). Scanning electron microscopy (SEM) was used to characterize biomass. Studying adsorption was done in batches. The study included kinetics, thermodynamics, and adsorption isotherms. The outcomes shown that over a 24-hour contact period, (SCB) exhibited a maximum adsorption capacity of 9.41 mg/g at 45 ºC. The pseudo-second order model was better suited by adsorption kinetics data, suggesting a chemical mechanism was at work. The data acquired for the adsorption isotherms might be adjusted more effectively using the three-parameter Sips's isotherm model, suggesting a heterogeneous adsorption process. The technique proved to be viable, spontaneous, and endothermic. Consequently, it was determined that (SCB) showed promise as a biosorbent material for the remediation of waterways tainted by (MB).

In 2019, Silvia Alvarez-Torrellas, et. al. [24], created and described a novel adsorbent bead of alginate (A)/maghemite nanoparticles (γ-Fe_2O_3)/functionalized multiwalled carbon nanotubes (f-CNT) using a variety of methods, such as N_2 adsorption-desorption isotherms, and evaluated it further for the ability to adsorb the dye methylene blue (MB) from solutions. It took an estimated 48 hours to reach the equilibrium of (MB) adsorption onto the beads. In order to fit the kinetic and equilibrium experimental data, a number of kinetic and isotherm equation models were applied. The monolayer model was used to quantify the number of adsorbed (MB) molecules per active site, the anchoring number, the density of receptor sites, the adsorbed quantity at saturation, the concentration at half saturation, and the molar adsorption energy. The adsorption process appeared to be spontaneous and endothermic based on the computed negative ΔG^o and positive ΔH^o values.

In 2016, Robati, et. al. [25], employed the effective nanocomposite Multi-Walled Carbon Nanotube Functionalized Thiol (MWCNT-SH) as an adsorbent to quickly remove the dangerous cationic dye methylene blue from the liquid phase and quickly adsorb it. It was discovered that when the starting concentrations of (MB) dye are increased from 10 to 40 mg/L, the adsorption capacity improves as well. Additionally, it was discovered that the adsorption equilibrium data for MWCNT, MWCNT-SH1, MWCNT-SH3, and MWCNTS-SH5 were well fitted and in good agreement with the Langmuir isotherm model type (III), Freundlich isotherm model, and Langmuir isotherm model type (II), respectively.

Materials and Methods

Graphene Oxide (GO) Synthesis

Graphene Oxide (GO) was produced from organic graphene powder using an enhanced and minimally altered method. A solution of hydrochloric acid (H_2SO_4) and a solution of hydrogen peroxide (H_3O_3) were generally mixed in a flask at a volume/volume ratio of (9:1). A gradual addition of this concentrated acid mixture was made to a homogenous solid mixture containing 1.8 grammes of potassium permanganate ($KMnO_4$) and 0.3 grammes of graphite, which was maintained in a water bath. Then, after 12 hours of stirring at 50 ºC and the completion of the graphite oxidation process, the reaction mixture turned dark brown [26]. Immediately upon the reaction mixture's arrival at room temperature, 500 mL of ice-cold water were added. Subsequently, a progressive addition of 30% hydrogen peroxide (H_2O_2) was made until the reaction mixture's colour changed to an intense yellow. After the filtrate was centrifuged, the solid material was repeatedly cleaned as part of the workup procedure using water, 30% hydrochloric acid (HCl), and ethanol. The dark-brown crystalline powder was vacuum-dried at room temperature and then dried in a desiccator [27] [28]. Figure 1 shows the synthesis of graphene oxide (GO).

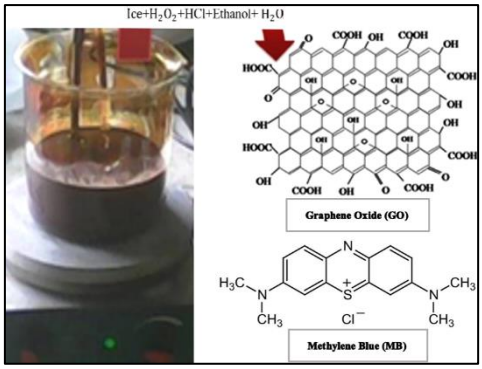

Figure 1: Synthesis of Graphene Oxide (GO).

Nickel Oxide/Cerium Oxide/Graphene Oxide ($NiO/CeO_2/GO$) Synthesis

First, using Hummer's method, natural graphite powder (GO) was made. Next, using an ultrasonic stirrer, (GO) was dissolved in 100 mL of distilled water for 30 minutes. Second, 60 mL of distilled water was used to dissolve 0.3 M of nickel (II) nitrate ($Ni(NO_3)_2$) and 0.3 M of cerium (III) chloride (($NCeCl_3$)), which were then stirred for an hour. Finally, after adding sodium hydroxide (NaOH) to bring the mixture's pH to 7, it was heated for 24 hours at 180 ºC inside a hydrothermal Teflon liner. The finished product was dried in a vacuum oven at 60 ºC for eight hours after being regularly cleaned with distilled water and ethanol [29].

Results and Discussion

The Effect of Initial Dye Concentration

The initial concentrations of $NiO/CeO_2/GO$ have an impact on the reactive Methylene Blue (MB) dye adsorption phenomena. The impact of different $NiO/CeO_2/GO$ concentrations (0.25-1.0 mg/L) is shown in Figure 2. The treated (MB) dye was found to exhibit the saturation point for $NiO/CeO_2/GO$ at 1.0 mg/L. As the concentration of $NiO/CeO_2/GO$ was elevated until the saturation point was achieved, the dye uptake increased. This happened because of the increased pushing power of the concentration gradient [6]. The greatest amount of dye adsorbed per gramme at 1.0 mg/L, 25 °C for approximately 40 minutes at pH 7 was 105.26 mg/g for (MB) dye [30].

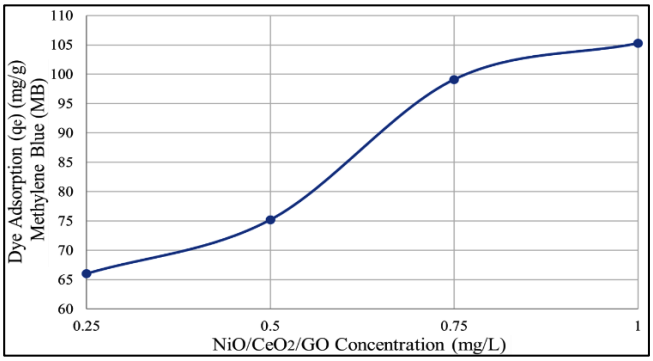

Figure 2: The Impact of Different $NiO/CeO_2/GO$ Concentrations.

Equilibrium Adsorption

Adsorption equilibrium times vary depending on the substance to be adsorbed as well as each adsorbent. This indicates the time it takes the adsorbent to reach maximum adsorption, which is a crucial component in adsorption experiments. The findings of the kinetic analysis for the adsorption of (MB) dye are shown in Figure (3).

Based on the acquired data, it was noted that the equilibrium was attained quickly and that the removal speed was rapid. This may be explained by the presence of several active sites, including ethers, asters, carbonyl, alcohol, and phenol groups, oxygen groups, and carbonyl groups that suggested positively charged (MB), on the surface of $NiO/CeO_2/GO$ at the beginning of the adsorption process. Due to adsorbent site saturation and electrostatic interference between positively charged adsorbed species, which lowers the adsorption rate, there is a rapid adsorption phase followed by a slow adsorption phase [31].

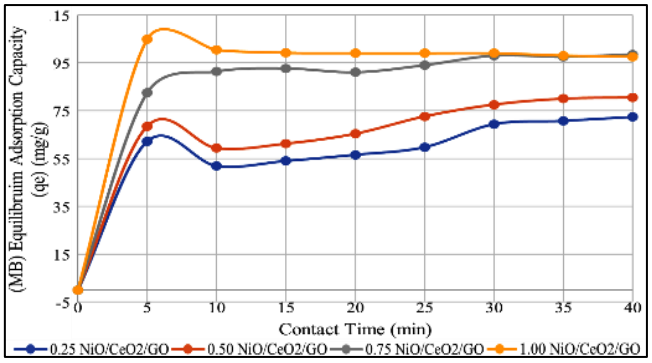

Figure 3: The Kinetic Analysis for the Adsorption of (MB) Dye.

Adsorption Kinetics

The efficiency of sorption is defined by the residence time of the sorption reaction, which is controlled by the rate of solute adsorption, which is described by sorption kinetics [32]. The pseudo-first- and pseudo-second-order kinetic models are the most often utilized.

Pseudo-First-Order

The pseudo-first-order equation for calculating the rate of adsorption was developed by Lagregren in 1898. Equation (1) provides the adsorption rate:

$$\frac{dqt}{dt} = (qe - qt) \tag{1}$$

Where, qe is the equilibrium adsorption capacity of (MB) dye and qt is the adsorption capacity of (MB) dye at certain time (t). After integration with boundary conditions from t = 0 to t = t and qt = 0 to qt = qt, the equation takes on the following linear form:

$$\log\ (qe - qt) = \log qe - \frac{k_1}{2.303} t \tag{2}$$

Where, k_1 is the pseudo-first-order adsorption kinetic of the (MB) dye (1/min). If the kinetic data correlate with pseudo-first-order, the values of qe and k_1 at various beginning concentrations can be computed using the slope and intercept of the log (qe - qt) vs t plots, which produce a straight line [33].

Pseudo-Second-Order

Equation (3) provides the pseudo-second-order adsorption rate:

$$\frac{dqt}{dt} = k_2 (qe - qt)^2 \tag{3}$$

Where, k_2 is the pseudo-second-order adsorption kinetic of the (MB) dye (g/mg.min). After both sides are integrated from t = 0 to t = t and qt = 0 to qt = qt, the boundary conditions are applied, and the integrated version of the equation is as follows:

$$\frac{t}{qt} = \frac{1}{k_2\, qe^2} + \frac{1}{qe} t \tag{4}$$

A linear plot of t (time) Vs t/qt can be used to derive the rate constant k_2 and equilibrium adsorption capacity qe [34] [35]. Table (1) shows the values of equilibrium adsorption capacity of (MB)dye, the pseudo-first-order adsorption kinetic of the (MB) dye (k_1) and the pseudo-second-order adsorption kinetic of the (MB) dye (k_2) for various NiO/CeO_2/GO original concentrations (Co). Figures 4A and 4B displays the adsorption kinetics data that were fitted into the pseudo-first-order and pseudo-second-order kinetics models respectively. Table 1 and 2 provides the (MB) dye parameters values that were determined at various contact time (5 – 40 minutes).

The correlation coefficients (R^2) for the NiO/CeO_2/GO concentrations of 0.25, 0.50, 0.75, and 1.00 mg/L, respectively, for the pseudo-first-order, as shown in Figure 4A, are (0.9903, 0.9670, 0.9997, and 0.9997). This was

achieved by plotting log(qe-qt) against the time (t). These results demonstrate that the adsorption process fits the pseudo-first-order reasonably well. Since the correlation coefficients (R^2) values for the $NiO/CeO_2/GO$ concentrations (0.25, 0.50, 0.75, and 1.00 mg/L) were (0.9697, 0.9870, 0.9989, and 0.9997), the linear plot of (t/qt) versus the time (t) in Figure 4B for the pseudo-second-order showed a good agreement that the adsorption process was fit. As a result, the maximum (R^2) values of the pseudo-first-order and pseudo-second-order kinetic models at $NiO/CeO_2/GO$ concentration (1.00 mg/L) showed that both kinetic models could be applied to explain the adsorption of $NiO/CeO_2/GO$ on (MB) dye.

Table 1: Pseudo-First-Order and Pseudo-Second-Order Adsorption Kinetic of the (MB) Dye

$NiO/CeO_2/GO$ Concentration (Co) (mg. L^{-1})	(MB) Equilibrium Adsorption Capacity (qe) (mg. g^{-1})	Pseudo-First-Order Kinetics (k_1) (min^{-1})	R^2	Pseudo-Second-Order Kinetics (k_2) ($g.mg^{-1}.min^{-1}$)	R^2
0.25	62.06	0.132	0.9903	0.003	0.9697
0.50	70.62	0.262	0.9670	0.008	0.9870
0.75	93.19	0.422	0.9997	0.018	0.9989
1.00	99.61	0.428	0.9997	0.015	0.9997

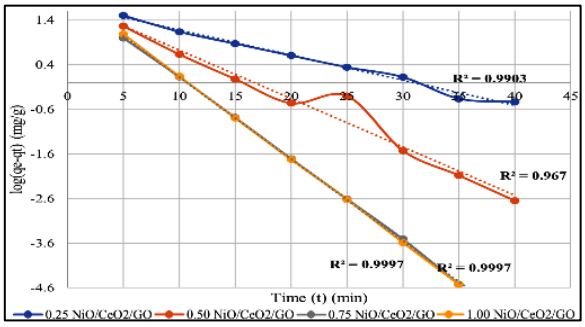

Figure 4A. Pseudo-First-Order Kinetics

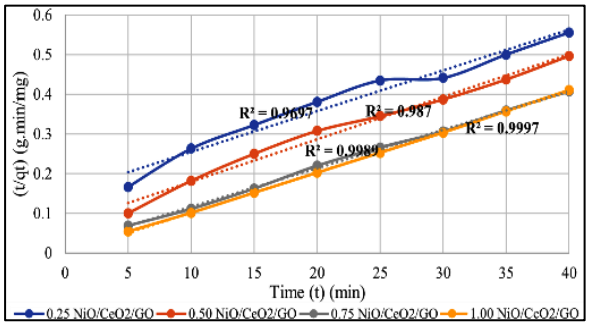

Figure 4B. Pseudo-Second-Order Kinetics

Table 2: (MB) Dye Parameters Values.

$NiO/CeO2/GO$ (Co) (mg/L)	(MB) Parameter	Time 05 (min)	Time 10 (min)	Time 15 (min)	Time 20 (min)	Time 25 (min)	Time 30 (min)	Time 35 (min)	Time 40 (min)
0.25	Ce (mg/L)	00.18	00.16	00.13	00.12	00.11	00.08	00.08	00.07
	qe (mg/g)	62.09	51.85	53.95	56.53	59.70	69.32	70.70	72.37
	qt (mg/g)	30.00	38.00	46.50	52.50	57.50	68.00	70.00	72.00
0.50	Ce (mg/L)	00.25	00.23	00.20	00.18	00.14	00.11	00.10	00.10
	qe (mg/g)	68.48	59.38	61.20	65.38	72.60	77.53	80.01	80.50
	qt (mg/g)	50.00	55.00	60.00	65.00	72.50	77.50	80.00	80.50
0.75	Ce (mg/L)	00.21	00.08	00.06	00.07	00.05	00.02	00.02	00.01
	qe (mg/g)	82.50	91.34	92.67	91.02	94.00	98.00	97.50	98.50
	qt (mg/g)	72.50	90.00	92.50	91.00	94.00	98.00	97.50	98.50
1.00	Ce (mg/L)	00.08	00.01	00.01	00.01	00.01	00.01	00.02	00.03
	qe (mg/g)	104.83	100.40	99.16	99.02	99.00	99.00	98.00	97.50
	qt (mg/g)	92.50	99.00	99.00	99.00	99.00	99.00	98.00	97.50

Assuming that the pseudo-first- and pseudo-second-order kinetic models fit the data successfully, it can be proposed that chemisorption was the rate-limiting step of the adsorption speed control involving valance forces through the sharing or exchanging of electrons between the (MB) dye and $NiO/CeO_2/GO$ [36].

Modelling of Adsorption Isotherms

The graph that represents the quantity of product adsorbed per initial mass of adsorbent at the concentration that remains in the solution after adsorption equilibrium is known as the adsorption isotherm. It is bound at a specific temperature. The adsorption isotherm offers vital information about the dynamics of the equilibrium interactions between the adsorbate molecules and the adsorbent surface, as well as the adsorbent's adsorption capacity, efficacy, and orientation of the adsorbate molecules on the surface. Regarding elucidating the adsorption mechanism, these are also very significant [37].

Plotting the concentrations of solid phases versus concentrations of liquid phases provides a graphic description of the equilibrium adsorption isotherm. In order to better understand the adsorption process, numerous equilibrium isotherm models have been developed over time, including the Langmuir, Freund, Brunauer–Emmett–Teller, Redlich–Peterson, Dubinin–Radushkevich, Temkin, Toth, Koble–Corrigan, Sips, Khan, Hill, Flory–Huggins, and Radke–Prausnitz isotherm [38]. The Langmuir, Freundlich, Tempkin, and Dubinin-Radushkevich isotherm models are the most often used ones [39].

Langmuir Isotherm Model

According to the Langmuir model, identical homogeneous spots on a solid surface experience monolayer sorption. Additionally, it implies that once the active sites are coated with dye molecules, no more adsorption occurs. The following formula presents the saturated monolayer isotherm (The adsorbed molecules at the nearby adsorption sites do not interact with one another) [40] [41]:

$$\frac{Ce}{qe} = \frac{1}{b.qm} + \frac{1}{qm} Ce \quad (5)$$

Where, qe is the unit equilibrium adsorption capacity and qm is the maximum dye absorption, providing the information about adsorption capacity for a full monolayer (mg/g); Ce is the concentration of dye at equilibrium in solution (mg/L). If the Langmuir equation is followed by the adsorption equilibrium, the plot of Ce vs Ce/qe has a linear form. Figures 5A, 5B, 5C and 5D shows the Langmuir isotherm parameters for NiO/CeO_2/GO concentrations (0.25, 0.50, 0.75 and 1.00 mg/L) respectively.

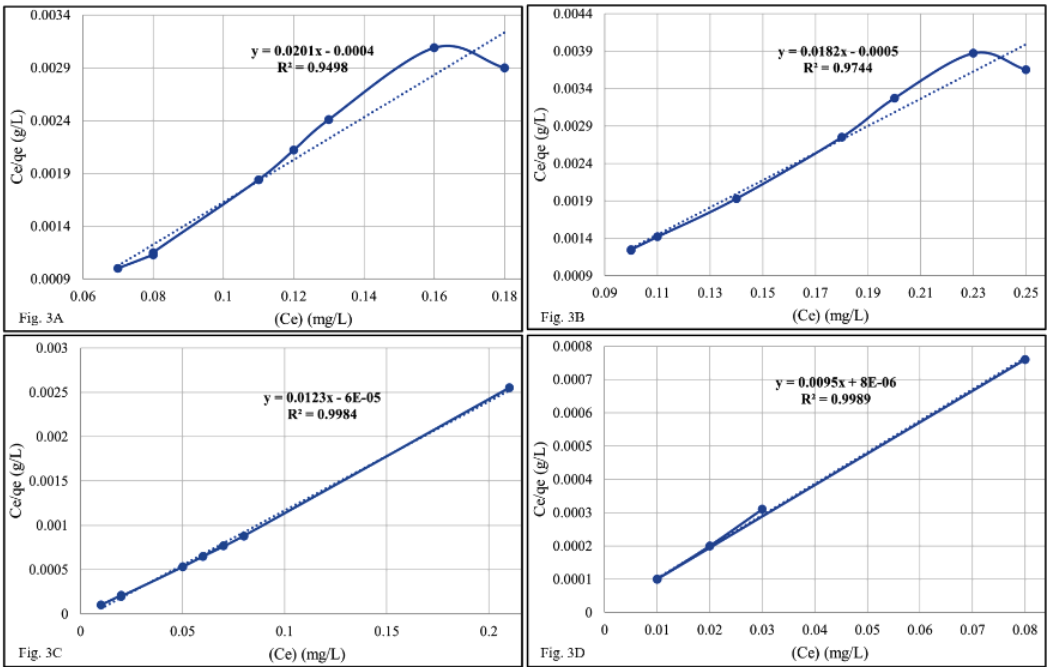

Figure 5A, 5B, 5C and 5D: Langmuir Isotherm Linearized Model for NiO/CeO_2/GO (0.25, 0.50, 0.75, and 1.00 mg/g) at 298 K and pH (7).

In the case of the four NiO/CeO_2/GO composites concentrations for (MB) dye adsorption, a reasonable agreement of correlation coefficient values (R^2) of the Langmuir isothermal model was obtained based on the experimental data. The concentrations of 1.00 mg/L (R^2 = 0.9989), 0.75 mg/L (R^2 = 0.9984), 0.50 mg/L (R^2 = 0.9744), and 0.25 mg/L (R^2 = 0.9498) all more closely fitted the adsorption data. An increase in adsorption with increasing NiO/CeO_2/GO concentration is indicative of (MB) dye adsorption on NiO/CeO_2/GO on homogenous surfaces.

Freundlich Isotherm Model

The process of adsorption from wastewater for organics and heavy metals is often described by the Freundlich equation, an empirical equation. Multilayer or heterogeneous adsorption sites serve as its foundation [42] [43]. Additionally, it suggests that the stronger binding sites are occupied before the lesser ones and that the adsorption strength diminishes with increasing degree of occupation [39]. The Freundlich equation has the following linear form:

$$\log qe = \log K + \frac{1}{n} \log Ce \quad (6)$$

Where, the Freundlich constants are denoted by K and n. If the value of 1/n is below the unit, the adsorption process is chemical; if the value is above the unit, the more physical adsorption occurs; the more heterogeneous the surface, the closer the value of 1/n gets to zero [43]. The plot of logqe vs logCe has a linear form.

Figures 6A, 6B, 6C and 6D shows the Freundlich isotherm parameters for $NiO/CeO_2/GO$ concentrations (0.25, 0.50, 0.75 and 1.00 mg/L) respectively.

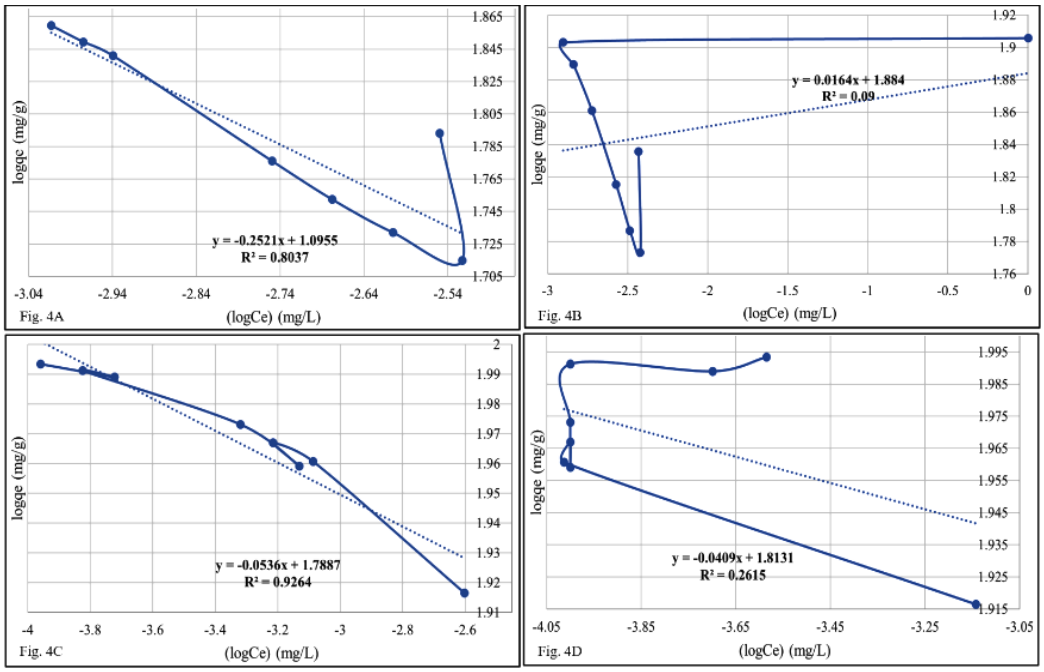

Figure 6A, 6B, 6C and 6D. Freundlich Isotherm Linearized Model for $NiO/CeO_2/GO$ (0.25, 0.50, 0.75, and 1.00 mg/g) at 298 K and pH (7).

According to the correlation coefficient (R^2) of the Freundlich isothermal model in Figures 4A, 4B, 4C, and 4D. $NiO/CeO_2/GO$ composite concentration (1.00 mg/L) (R^2 = 0.8073), 0.75 mg/L (R^2 = 0.0900), 0.50 mg/L (R^2 = 0.9264), and 0.25 mg/L (R^2 = 0.2615).

The Freundlich isotherm's (R^2) values showed that this model is not as well suited to the current system. The greatest (R^2) value for the Freundlich model was achieved at 0.75 mg/L of $NiO/CeO_2/GO$ when compared to 0.25, 0.50, and 1.00 mg/L of applied concentration. The 0.75 mg/L indicates that the surface of $NiO/CeO_2/GO$ was comparatively more homogeneous. For $NiO/CeO_2/GO$ concentrations of 0.25, 0.50, 0.75, and 1.00 mg/L, respectively, the values of 1/n in the current study were 1.0955, 1.8840, 1.7887, and 1.8131. The adsorption process was physical in nature since the values of 1/n were greater than unity.

Dubinin–Radushkevich Isotherm Model

By using the sorption energy value, the Dubinin-Radushkevich isothermal model is utilized to forecast the kind of adsorption process, such as chemical or physical [44]. Equation describes the model in its linear form is:

$$\ln qe = \ln qmax - B\,\varepsilon^2 \quad (7)$$

Where, qmax is the highest concentration of pollutants that can be adsorbed on $NiO/CeO_2/GO$ and ε is the Polanyi potential, which has the following calculational formula:

$$\ln qe = RT \ln\left(1 + \frac{1}{Ce}\right) \varepsilon^2 \quad (8)$$

There is a linear form to the lnqe vs. ε^2 plot. When an adsorbate molecule is moved from infinity in the solution to the surface of the material, the constant B (mol^2 / kJ^2) yields the mean free energy E of adsorption per molecule and may be calculated using the following connection [45]:

$$E = \frac{1}{2\sqrt{B}} \tag{9}$$

The E (kJ/mol) value provides chemical or physical sorption type information. If E is less than 8 kJ/mol the adsorption process is physical in nature, while the adsorption process is chemical in nature if E value falls between 8 and 16 kJ/mol [46]. For the concentrations of NiO/CeO_2/GO (0.25, 0.50, 0.75, and 1.00 mg/L), the values of E in the current study were (1.366, 1.487, 1.487, and 1.529 kJ/mol), respectively. Hence, the adsorption process was physical in nature because the values of E were less than 8 kJ/mol.

Based on the Dubinin-Radushkevich isothermal model's correlation coefficient (R^2), as shown in Figures 7A, 7B, 7C, and 7D. 1.00 mg/L ($R^2 = 0.6127$), 0.75 mg/L ($R^2 = 0.8308$), 0.50 mg/L ($R^2 = 0.7562$), and 0.25 mg/L ($R^2 = 0.6009$) of NiO/CeO_2/GO composite concentration. In terms of fit, the Dubinin-Radushkevich isotherm is more closely aligned with the Freundlich isotherm and less closely aligned with the Langmuir isotherm (R^2 values).

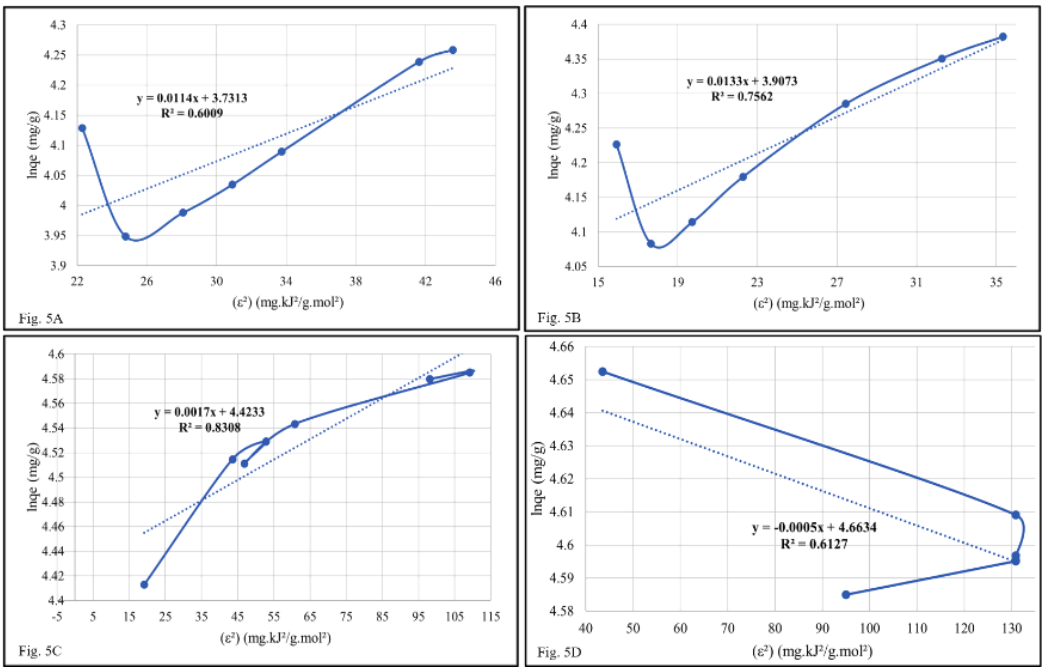

Figure 7A, 7B, 7C and 7D: Dubinin–Radushkevich Isotherm Linearized Model for NiO/CeO_2/GO (0.25, 0.50, 0.75, and 1.00 mg/g) at 298 K and pH (7).

The Langmuir model more accurately depicts the adsorption process of (MB) dye by the NiO/CeO_2/GO because its correlation coefficient (R^2) value is larger than that of the Freundlich and Dubinin–Radushkevich isotherms, which may point to the existence of a homogenous surface, very efficient adsorbate-adsorbent interactions, and extremely successful monolayer adsorption.

Adsorption of (MB) Dye: Thermodynamic Characteristics

The Gibbs free energy ΔG°, standard enthalpy ΔH°, and entropy ΔS° are the thermodynamic parameters of the adsorption, they were determined by applying the following formulas:

$$\Delta G^\circ = -RT \ln K_L \tag{7}$$

$$\ln K_L = \frac{\Delta S^\circ}{R} - T\,\Delta H^\circ \tag{8}$$

$$\Delta G^\circ = \Delta H^\circ - T\,\Delta S^\circ \tag{9}$$

Where T is the temperature (K), K_L is the Langmuir constant, and R is the ideal gas constant (kJ/mol.K) [47], [48].

Table 3 shows the thermodynamic calculations' findings. The spontaneous nature of the adsorption process is demonstrated by the negative value of the Gibbs free energy (ΔG°) for (MB) dye adsorption. With a low value of (ΔH°) between 0.020 and 0.032 kJ/mol, the adsorption process appears to be endothermic overall. These (ΔH°)

values can be explained by the relatively strong contact between the NiO/CeO_2/GO ions and the (MB) surface. The well solvated nature of the (MB) dye ions is one explanation for positive (ΔH^o).

Table 3 further demonstrates that the (ΔS^o) value, which varies from 0.051 to 0.073 kJ/mol.K, was positive. The redistribution of energy between the (MB) dye and the NiO/CeO_2/GO is the cause of this. There will be more ordered heavy metal ions close to the (MB) dye surface before to adsorption than there will be in the ensuing adsorbed state, and there will be a larger ratio of free heavy metal ions to ions interacting with the (MB) dye.

Consequently, randomness will rise at the solid–solution interface during the adsorption process, and the distribution of rotational and translational energy among a small number of molecules will grow with increased adsorption by producing a positive value of (ΔS^o). Because (ΔH^o) > 0 and (ΔS^o) > 0, adsorption is therefore likely to happen spontaneously at normal and high temperatures [49].

Ultimately, the relatively tiny and positive enthalpy shift suggests that the interactions are mostly physical and the adsorption is endothermic in nature. However, the little and positive entropy change may also be explained by the partial rise in disorder brought on by the adsorption-induced dehydration of hydrated dye ions.

Table 3: Thermodynamics Parameters of (MB) Dye Adsorption.

NiO/CeO_2/GO Concentration (Co) (mg. L^{-1})	$\ln K_L$	Thermodynamics Parameters		
		$\Delta G°$ kJ.mol^{-1}	$\Delta H°$ kJ.mol^{-1}	$\Delta S°$ kJ. $mol^{-1}.K^{-1}$
0.25	-2.02495	-15.31	0.021	0.051
0.50	-1.33941	-15.07	0.020	0.051
0.75	-0.86275	-19.10	0.029	0.064
1.00	-0.84863	-21.66	0.031	0.073

Comparison of adsorption Kinetics

Finally, the adsorption information reported for similar or closer adsorbent-adsorbate systems in the literature were compared with the highest possible adsorption capacity, the correlation coefficients of the applied isotherm models, and the thermodynamics parameters (ΔG°, ΔH°, and ΔS°) for (MB) dye absorption on the NiO/CeO_2/GO composite surface in this study. The Performance comparison of several adsorbents for methylene blue removal from aqueous solutions is shown in Table (4).

Table 4: The Performance Comparison of Several Adsorbents for Methylene Blue (MB) Removal from Aqueous Solutions.

Ref.	Adsorbent	Maximum Adsorption (mg/g)	Isotherm Models-R^2	Thermodynamics Parameters		
				$\Delta G°$ kJ.mol^{-1}	$\Delta H°$ kJ.mol^{-1}	$\Delta S°$ kJ. $mol^{-1}.K^{-1}$
[17]	This Work	105.26	L-0.9989, F-0.9264, DR-0.8303	-21.66	0.0310	0.0730
[18]	Activated Carbon	0.00096	L-0.080, F-0.971, T-0.754	-9.751	-0.740	-0.002
[19]	Manganese Oxide at Reduced Graphene	156	L-0.9901, F-0.9128, DR-0.7851, RP-0,9465	-3.89	26.830	0.063
[21]	Humic acid, Biochar, Silica	16.23	L-0.980, F-0.896, T-0.830	-24.15	6.380	0.030
[22]	Nickel Oxide, Silica	124	L-0.982, F-0.898, T-0.870	-2.858	-14.455	-38.683
[23]	Hydroxyapatite, Gold	200	L-0.992, F-0.871	-6.050	33.300	0.134
[24]	Carboxymethyl Cellulose	18.52	L-0.964, F-less than L	-2.820	5.540	19.140
[25]	Sugarcane Bagasse	9.41	L-0.9329, F-09128, S-0.9703, T-0.937	-18.04	1.930	0.066
[26]	Maghemite, Carbon Nanotube	320.5	L-0.977, F-0.907, S-0.999	-20.2	36.900	0.195

* L= Langmuir, F= Freundlich, DR= Dubinin–Radushkevich, T=Temkin, S=Sips, T-Toth, RP=Redlich-Peterson.

Conclusions

The application of the Nickel Oxide/Cerium Oxide/Graphene Oxide (NiO/CeO2/GO) nanocomposite as a long-term adsorbent for the elimination of (MB) dye from aqueous solution is demonstrated by this work.

Langmuir, Freundlich, and Dubinin-Radushkevich isotherms could be used to characterize the adsorption. The maximal adsorption capacity was 105.26 mg/g at 1.0 mg/L, 25 °C for about 40 minutes at pH (7).

It was seen from the collected data that both the equilibrium and the removal speed were reached swiftly. The Langmuir isotherm had the best correlation coefficients (R^2), which may point to the existence of a homogenous surface, very efficient adsorbate-adsorbent interactions, and extremely successful monolayer adsorption.

The results of kinetic investigations indicate that the (MB) dye removal kinetics are best described by the pseudo-first-order and pseudo-second-order models, with intraparticle diffusion control also being an efficient adsorption mechanism.

The thermodynamic analysis demonstrated that, within the temperature range under consideration, the adsorption of (MB) dye onto activated carbon was spontaneous (negative ΔG^o) and endothermic (positive ΔH^o).

The results enhance our knowledge of the adsorption process and its possible uses in the treatment of wastewater from (MB) dye contaminations.

References

[1] Lin, K. & Zhao, H. “The Impact of Green Finance on the Ecologicalization of Urban Industrial Structure-Based on GMM of Dynamic Panel System”. J. Artif. Intell. Technol. 2, 123-129-2022.

[2] Mehra, S., Singh, M. & Chadha, P. “Adverse Impact of Textile Dyes on the Aquatic Environment as well as on Human Beings”. Toxicol. Int. 28, 165-2021.

[3] Khan, S. & Malik, A. “Environmental and Health Effects of Textile Industry Wastewater” DOI 10.1007/978-94-007-7890-0, pp. 55-71-2014.

[4] Ribeiro, M. R. et al. “Synthesis of Value-Added Materials from the Sewage Sludge of Cosmetics Industry Effluent Treatment Plant.” J. Environ. Chem. Eng. 9, 105367-2021.

[5] Tshimangadzo S. Munonde, et. al. “Two Agitation Routes for the Adsorption of Reactive Red 120 Dye on NiFe LDH/AC Nanosheets from Wastewater and River Water” Journal of Applied Clay Science, Volume 219-106438, 15 March 2022.

[6] Asghar Hamzezadeh, et. al. “Application of Low-Cost Material for Adsorption of Dye from Aqueous Solution” International Journal of Environmental Analytical Chemistry, Volume 102-Issue 1-2022.

[7] Dan Zhang, et. al. “Green Synthesis of Metallic Nanoparticles and their Potential Applications to Treat Cancer” Journal of Front Chemistry, DIO: 10.3389/fchem-0079-2020.

[8] Ravishankar T. N., et. al. “Synthesis and Characterization of CeO_2 Nanoparticles via Solution Combustion Method for Photocatalytic and Antibacterial Activity Studies” ChemistryOpen Journal, DOI: 10.1002/open.201402046, 4:146-154-2015.

[9] Hassan T., et. al. “Functional Nanoparticles and their Potential Applications: A Review, Journal of Polymer Research, 28-2:1-22-2012.

[10] Olak-Kucharczyk, M., Szczepańska, G., Kudzin, M. H. & Pisarek, M. The Photocatalytical Properties of RGO/TiO_2 Coated Fabrics. Coatings 10, 1041-2020.

[11] Sedaghat, S. “Synthesis of Clay–CNTs Nanocomposite. J. Nanostruct. Chem. 3, 24-2013.

[12] Dreyer, D.R., Park, S., Bielawski, C., Ruoff, R.S. “The Chemistry of Graphene Oxide. Chem. Soc. Rev. 39, 228-240-2010.

[13] Huang, L., et. al. “Study on Synthesis and Antibacterial Properties of Ag NPs/GO Nanocomposites. J. Nanomater, 5685967-2016.

[14] Czepa, W., et. al. “Graphene Oxide-Mesoporous SiO_2 Hybrid Composite for Fast and Efficient Removal of Organic Cationic Contaminants” Elsevier, 158, 193-201-2020.

[15] O. Hamdaoui, E. Naffrechoux “Modeling of Adsorption Isotherms of Phenol and Chlorophenols onto Granular Activated Carbon: Part I. Two-parameter models and Equations Allowing Determination of Thermodynamic Parameters” J. Hazard Mater. 147, 381-394-2007.

[16] X. Tang, G. Ran, J. Li, Z. Zhang, C. Xiang “Extremely Efficient and Rapidly Adsorb Methylene Blue Using Porous Adsorbent Prepared from Waste Paper: Kinetics and Equilibrium Studies” J. Hazard Mater. 402, 123579-2021.

[17] Mohammed A. Al-Madani, Faraj M. Al-Lafi “Synthesis of Nickel Oxide/Cerium Oxide/ Graphene Oxide (NiO/CeO_2-GO) composites as an Organic Remover Pollutant of Dyes” Journal of Pure and Applied Sciences, DIO: 10.51984/JOPAS. V22I3. 2999, Volume: 22 No.3, 2023.

[18] Atef El Jery, et. al. “Isotherms, Kinetics and Thermodynamic Mechanism of Methylene Blue Dye Adsorption on Synthesized Activated Carbon” Department of Chemical Engineering, College of Engineering, King Khalid University, 61411 Abha, Saudi Arabia, Scientific Reports:14:970-2024.

[19] Tshimangadzo S. Munonde, et. al. “Removal of Methylene Blue Using Mno2@rGO Nanocomposite from Textile Wastewater: Isotherms, Kinetics and Thermodynamics Studies” Heliyon Journal, Volume 9, Issue 4, E15502, April 2023.

[20] Abbas M Abbas, et. al. “Preparation and Characterization of Eco-Friendly Nanocomposite for Methylene Blue Dye Removal from Industrial Wastewater” Chemistry Department, Faculty of Science, Suez Canal University. Ismailia, 41522, Egypt, Journal of Advances in Environmental and Life Sciences 2: 32-43-2022.

[21] Davoudi and Shahnaz “Adsorption of Methylene Blue (MB) Dye Using NiO-SiO_2NPs Synthesized from Aqueous Solutions: Optimization, Kinetic and Equilibrium Studies” Department of Chemistry Omidiyeh Branch, Islamic Azad University, Omidiyeh, I.R. Iran, Iran. J. Chem. Chem. Eng., Vol. 41, No. 7-2022.

[23] Kashma Sharma, et. al. “Methylene Blue Dye Adsorption from Wastewater Using Hydroxyapatite/Gold Nanocomposite: Kinetic and Thermodynamics Studies” Nanomaterials Journal, 11-1403-2021.

[23] W. A. Albokheet, et. al. “Removal of Methylene Blue Dye Using Nickel Oxide/ Carboxymethyl Cellulose Nanocomposite: Kinetic, Equilibrium and Thermodynamic Studies” Department of Chemistry, King Faisal University, Saudi Arabia, Journal of Textile Science & Fashion Technology, ISSN: 2641-192X, DOI: 10.33552/JTSFT.2021.08.000685, 2021.

[24] Thaisa Caroline Andrade Siqueira “Sugarcane Bagasse as an Efficient Biosorbent for Methylene Blue Removal: Kinetics, Isotherms and Thermodynamics” Int. J. Environ. Res. Public Health, 17, 526; DOI:10.3390/ijerph17020526, 2020.

[25] Silvia Alvarez-Torrellas, et. al. “Effective Adsorption of Methylene Blue dye onto Magnetic Nanocomposites. Modeling and Reuse Studies, Catalysis and Separation Processes Group (CyPS)” Chemical Engineering and Materials Department, Faculty of Chemistry Sciences” Journal of Appl. Sci., 9-4563; DOI:10.3390/app9214563, 2019.

[26] Robati, et. al., Adsorption Behavior of Methylene Blue Dye on Nanocomposite Multi-Walled Carbon Nanotube Functionalized Thiol (MWCNT-SH) as New Adsorbent” Journal of Molecular Liquids, Volume 216, Pages 830-835-April 2016.

[27] Marcano, D.C., et. al. “Improved Synthesis of Graphene Oxide. ACS Nano Journal, 4, 4806-4814-2010.

[28] Emiru, T. F. and Ayele D. W. “Controlled Synthesis Characterization and Reduction of Graphene Oxide: A Convenient Method for Large Scale Production” Egyptian Journal of Basic and Applied Sciences, Volume 4, No. 1, pp. 74-97, 2017.

[29] Sonam V. Saacheti, et. al. “Synthesis of Ultrasound Assisted Nanostructured (NIO Support over CeO2) as well as Sonocatalytic Dye Degradation” Chemical Engineering Journal, Elsevier, ISSN: 1385-8974, 2023.

[30] Rattanaphani S, et. al. “An Adsorption and Thermodynamic Study of Lac Dyeing on Cotton Pretreated with Chitosan” Dyes and Pigments Journal, 72(1):88-96-2007.

[31] Moubarik, A. and Grimi, N. “Valorization of Olive Stone and Sugar Cane Bagasse By-Products as Biosorbents for the Removal of Cadmium from Aqueous Solution” Food Res. Int. J., 73, 169-175, 2015.

[32] D. Onyancha, et. al. “Studies of Chromium Removal from Tannery Wastewaters by Algae Biosorbents, Spirogyra Condensata and Rhizoclonium Hieroglyphicum” J. Hazard. Mater., Volume 158, no. 2–3, pp. 605–614, DOI: 10.1016/j.jhazmat.2008.02.043, 2008.

[33] N. K. Mondal, et. al. “Enhanced Chromium (VI) Removal Using Banana Peel Dust: Isotherms, Kinetics and Thermodynamics Study,” Sustain. Water Resour. Manag., Volume 4, No. 3, pp. 489-497, DOI: 10.1007/s40899-017-0130-7-2018.

[34] R. S. Ingole, et. al. “Adsorption of Phenol onto Banana Peels Activated Carbon,” KSCE J. Civ. Eng., vol. 21, No. 1, pp. 100–110, DOI: 10.1007/s12205-016-0101-9-2017.

[35] A. Ali, K. Saeed, and F. Mabood “Removal of Chromium (VI) from Aqueous Medium Using Chemically Modified Banana Peels as Efficient Low-Cost Adsorbent” Alexandria Eng. J., Volume 55, No. 3, pp. 2933–2942, DOI: 10.1016/j.aej.2016.05.011-2016.

[36] Dadrasnia, A., et. al. “Biosorption Potential of Bacillus Salmalaya Strain 139SI for Removal of Cr (VI) from Aqueous Solution” Int. J. Environ. Res. Public Health, 12, 15321-15338-2015.

[37] Ahmet Gürses, et. al. “Investigation of the Removal Kinetics, Thermodynamics and Adsorption Mechanism of Anionic Textile Dye, Remazol Red RB, with Powder Pumice, A Sustainable Adsorbent from Waste Water” Front. Chem., Sec. Green and Sustainable Chemistry, Volume 11 – 2023.

[38] A. Malek and S. Farooq, “Comparison of Isotherm Models for Hydrocarbon Adsorption on Activated Carbon” AIChE, J., Volume 42, No. 11, pp. 3191–3201, DOI: 10.1002/aic.690421120, 1996.

[39] V. M. Bhandari and V. V. Ranade, Advanced Physico-Chemical Methods of Treatment for Industrial Wastewaters, Elsevier Ltd., 2014.

[40] H. Hameed and A. A. Rahman “Removal of Phenol from Aqueous Solutions by Adsorption onto Activated Carbon Prepared from Biomass Material” J. Hazard. Mater., Volume 160, No. 2–3, pp. 576–581, DOI: 10.1016/j.jhazmat.2008.03.028, 2008.

[41] H. N. Bhatti, et. al. “Efficient Remediation of Zr (IV) Using Citrus Peel Waste Biomass: Kinetic, Equilibrium and Thermodynamic Studies” Ecol. Eng., Volume 95, pp. 216–228, DOI: 10.1016/j.ecoleng.2016.06.087, 2016.

[42] F. B. Liang, et. al. “Adsorption of Hexavalent Chromium on a Lignin-Based Resin: Equilibrium, Thermodynamics, and Kinetics” J. Environ. Chem. Eng., Volume 1, No. 4, pp. 1301–1308, DOI: 10.1016/j.jece.2013.09.025, 2013.

[43] A. Dada, et. al. “Langmuir, Freundlich, Temkin and Dubinin–Radushkevich Isotherms Studies of Equilibrium Sorption of $Zn^{(2+)}$ Unto Phosphoric Acid Modified Rice Husk,” IOSR J. Appl. Chem., vol. 3, No. 1, pp. 38-45, 2012.

[44] B. H. Hameed and A. A. Rahman “Removal of Phenol from Aqueous Solutions by Adsorption onto Activated Carbon Prepared from Biomass Material” J. Hazard. Mater., Volume 160, No. 2–3, pp. 576–581, DOI: 10.1016/j.jhazmat.2008.03.028, 2008.

[45] B. Singha and S. K. Das “Adsorptive Removal of Cu (II) from Aqueous Solution and Industrial Effluent Using Natural/Agricultural Wastes” Colloids Surfaces B Biointerfaces, Volume 107, pp. 97–106, DOI: 10.1016/j.colsurfb.2013.01.060, 2013.

[46] T. K. Naiya, et. al. “The Sorption of Lead (II) Ions on Rice Husk Ash,” J. Hazard. Mater., Volume 163, no. 2–3, pp. 1254–1264, DOI: 10.1016/j.jhazmat.2008.07.119, 2009.

[47] Mohan D. and Singh K. P. “Single- and Multi-Component Adsorption of Cadmium and Zinc Using Activated Carbon Derived from Bagasse: An Agricultural Waste” Water Res. 36: 2304-2318, 2002.

[48] Anirudhan T. S. and Radhakrishna P. G. “Chromium (III) Removal from Water and Waste Water Using a Carboxylate-Functionalized Cation Exchanger Prepared from a Lignocellulosic Residue” Journal of Colloid and Interface Science. 316: 268-276, 2007.

[49] J. A. Hefne, et. al. “Kinetic and Thermodynamic Study of the Adsorption of Pb (II) from Aqueous Solution to the Natural and Treated Bentonite” 11442, International Journal of the Physical Sciences · November 2008.